

## Parametric and Sensitivity Analysis on the Effects of Geotechnical Parameters on Tunnel Lining in Soil Surrounding

Mehrdad Mohammadifar<sup>1</sup>, Tohid Asheghi Mehmandari<sup>2</sup>, Ahmad Fahimifar<sup>3</sup>

1- Ms.c Student, Faculty of Civil and environmental Engineering, Amirkabir University of technology, Tehran, Iran

2- PhD Candidate, Faculty of Civil & Environmental Engineering, Amirkabir University of Technology, Tehran, Iran

3- Associate Professor, Faculty of Civil & Environmental Engineering, Amirkabir University of Technology, Tehran, Iran

### ABSTRACT

Facilities built in areas affected by earthquake activity, such as tunnels, which have always been an integral part of human life, must withstand both dynamic and static loading. It has led to the need for practical studies on the effects of earthquakes on underground structures and the factors affecting their destruction. For this purpose, in this research, at first different patterns of tunnel's excavation were investigated by using Plaxis 2D software and then based on Tabas earthquake in Iran, sensitivity dynamic analysis on geotechnical parameters of the soil surrounding tunnel such as cohesion, friction angle, unit weight and modulus of elasticity was carried out. As a result, the parameters whose changes have the greatest and least effects on the bending moment changes on the tunnel lining are introduced. The results showed that the bending moment of tunnel's lining is decreased by increasing the amount of cohesion, friction angle, and elasticity modulus of the soil surrounding the tunnel. But the maximum bending moment rises as the unit weight of earth around the tunnel increases. Also, modulus of elasticity of the soil surrounding tunnel has the most effect and cohesion changes have the least effect on bending moment induced on tunnel lining.

### ARTICLE INFO

**Receive Date:** 28 October 2023

**Revise Date:** 20 January 2024

**Accept Date:** 29 February 2024

### Keywords:

Tunneling

Numerical modeling

Sensitivity analysis

Geotechnical Parameters

All rights reserved to Iranian Society of Structural Engineering.

doi: <https://doi.org/10.22065/jsce.2024.422469.3250>

\*Corresponding author: Ahmad Fahimifar

Email address: Fahim@aut.ac.ir

## 1. Introduction

The construction and utilization of underground spaces, such as tunnels, have always been intrinsic to human existence, serving diverse purposes throughout history. To proactively manage the potential for irreversible risks, it is imperative to conduct meticulous evaluations of the structural stability of these constructions during the design phase, encompassing a comprehensive assessment of relevant geotechnical parameters. This comprehensive approach entails identifying and mitigating potential geotechnical damage, including ground settlement, displacement of tunnel ceilings, maximum axial forces and bending moment exerted on tunnel linings.

It is important to mention that the unrestrained impact of these factors might result in the development of fracture damages due to the emergence and propagation of cracks under applied loads within the surrounding overburden [1, 2]. The 1995 and 1999 earthquakes in Japan, Taiwan and Turkey, which significantly damaged mountain tunnels and underground metro system, were among the 1990s earthquakes that seriously damaged certain tunnels. This emphasizes how crucial it is to build tunnels properly to withstand dynamic loads like earthquakes [3].

Due to the fact that tunnels and underground structures are prone to seismic damage, numerous experimental, numerical, and laboratory research have been conducted, and valuable knowledge has been obtained. Based on researches, the type of ground (soil or rock) and its geotechnical properties, tunnel depth, shape and geometry, groundwater conditions, tunnel lining thickness and its stiffness, earthquake wave type and direction relative to the tunnel axis and other factors appear to influence earthquake intensity and destructive effects on underground structures.

In 2018, Chen and Sun used the OpenSees program to explore the influence of tunnel depth on seismic behavior of a rectangular cross-section metro station in Shenyang, China, with four different depths, under Dynamic loading on saturated soil. The results indicated that, by increasing the tunnel's depth, displacements of the tunnel induced by dynamic loads decreases. Furthermore, as the tunnel structure's depth increased, the fluctuations in pore water pressure reduced [4]. In this regard, Cilingir and Madabhushi compared the results of laboratory testing with finite element analysis and showed that the dynamic pressure of the ground increases with an increase in tunnel depth. Moreover, the maximum amount of dynamic pressure occurs at the crown of the tunnel [5].

The impact of changing the diameter of a circular tunnel on the bending moment and axial force applied to the tunnel lining was studied by Nahhasand and et al. They conducted a parametric investigation, and the findings, revealed that increasing the width of the tunnel increases both the bending moment and the axial force applied to the lining. In addition to increasing the diameter, increasing the maximum dynamic load, tunnel depth, and lining thickness increases the stress applied to the tunnel lining [6]. Tafik and et al. investigated criteria such as tunnel depth, lining thickness, and the type of soil surrounding the tunnel. The result showed that increasing the thickness of the tunnel lining plays a significant role in determining the forces and bending moments exerted on it [7]. Additionally, researchers have found that the interaction between the tunnel lining and the surrounding soil during dynamic waves is influenced by their relative stiffness. Specifically, as the stiffness ( $K$ ) and modulus of elasticity ( $E$ ) of the tunnel increase, the tunnel absorbs a greater amount of energy and force from the surrounding environment [7]. Cilingir and Madabhushi conducted laboratory studies using centrifuge testing to analyze the performance of rigid and flexible tunnels. They found that flexible tunnels exhibit improved low-frequency values when the tunnel is deep. The ratio of stiffening is greater for shallow tunnels compared to deep tunnels in rigid tunnels [8].

Furthermore, Naserkhani and Evan discovered through numerical modeling that increasing the maximum ground acceleration has greater impacts on shallow tunnels [9]. Chen et al. (2012) investigated the behavior of tunnels at various depths when subjected to seismic loads in 2012. In these simulations, the tunnel was subjected to S and P waves harmonically with frequencies of 3 Hz and 5 Hz. The results indicated that the effect of the S wave on the shear and bending stresses is much greater than that of the P waves. Also, as the harmonic load frequency increases, the stress values increase to some extent [10]. Liu et al. (2020) investigated the sensitivity of influencing factors to tunnel stability and the maximum main tensile stress on the inner surface of surrounding rock [11]. Minh and Nguyen (2022) studied the variations of the seismic stability number with changes in the horizontal earthquake acceleration coefficient were intensively investigated for different values of soil properties, internal friction angle and the depth-to-diameter ratio of the tunnel. It is shown that the seismic stability numbers of circular tunnels reduce remarkably with the increase of horizontal seismic coefficient and the soil weight [12].

According to previous researches, it seems that many numerical studies have been conducted by using simple constitutive models like Mohr-Coulomb for analyzing soil and rock surrounding the tunnel and under harmonic loads. So, it seems that new studies based on appropriate constitutive models and under seismic waves is needed. Hence, in this research, a sensitivity analysis based on a non-linear dynamic modeling approach was conducted to study the dynamic performance of tunnels using a hardening soil model with small strain constitutive behavior. By comprehensive review of previous research, it can be stated that the majority of studies have focused on parameters such as the shape, type, size of tunnels, and their lining characteristics. There have been very limited research on the influence of soil parameters on the forces and moments induced in the tunnel lining. Additionally, a probabilistic risk analysis method has been employed to obtain sensitivity functions and

factors .In this approach, sensitivity functions are derived from the outputs of numerical modeling, and sensitivity factors are then obtained based on mathematical and analytical relationships. Due to the complexities involved in dynamic loadings, harmonic loadings are often used in sensitivity analysis; however, in this research, actual earthquake accelerograms have been used as dynamic loadings. This type of loading is less commonly used by researchers due to the challenges in modeling and the significant time required for each dynamic analysis .

As previously stated, different factors such as cohesion, friction angle, soil elasticity modulus, and soil unit weight may all have an impact on the amount of forces and bending moments on the tunnel lining and its dynamic performance. As a result, using the Tabas seismic acceleration spectrum, sensitivity analysis was done on the tunnel's geotechnical parameters to investigate their influence on the amount of bending moment on the tunnel lining.

## 2-Assumption

### 2.1. Geometry and constitutive model

To ensure that the model’s boundaries have no noticeable effect on the results, the distance between the model’s boundary and the center of tunnel must be at least ten times the radius of the tunnel. The dimensions of the model and tunnel at a 20 m depth are shown in Fig. 1.

According to this fact that soils under dynamic loads exhibit nonlinear behavior in the range of small strains, hardening soil with small strain (HSS) constitutive model has been carried out to simulate the elastoplastic behavior of the soil surrounding the tunnel. The data in Table 1 relates to the findings of tests carried out on Tehran Metro Line 6. The groundwater level is assumed to be at the bottom of the model in every circumstance.

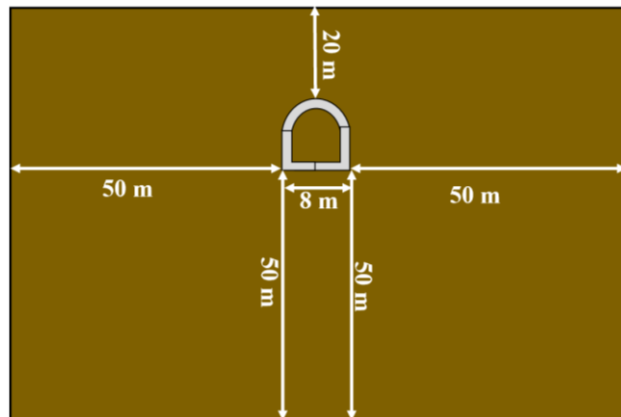


Figure 1. The geometry of a D-shaped tunnel.

Table 1. Soil properties [13]

| Type of Material | Density (kg/m <sup>3</sup> ) | Elastic Modulus (MPa) | Poisson's Ratio | Cohesion (KPa) | Internal Friction Angle (degrees) | Initial Shear Modulus (MPa) | Reference Shear Strain Soil |
|------------------|------------------------------|-----------------------|-----------------|----------------|-----------------------------------|-----------------------------|-----------------------------|
| soil             | 2000                         | 150                   | 0.3             | 60             | 30                                | 540                         | 0.00015                     |

### 2.2. Seismic Load and Damping properties

To investigate the dynamic performance of the tunnel under seismic loading, all models were analyzed using the 7.4 magnitude Tabas earthquake acceleration spectrum. The Tabas earthquake accelerogram spectrum is shown in Fig. 2. The physical damping resulting from viscous effects was considered by incorporating Rayleigh damping into the analysis. Proper modeling of the boundaries played a crucial role in the study. Special conditions were applied to prevent spurious wave reflections at the model boundaries, which do not occur in reality. Subsequently, a non-linear dynamic analysis based on the

hardening soil small strain constitutive model was conducted using Plaxis 2D software. The propagation of waves through the soil, considering the Tabas earthquake accelerogram spectrum, and its impact on the tunnel were investigated.

Eq. 1 determines the Rayleigh damping, which links a body's energy dissipation to its stiffness and mass matrices, to estimate damping in dynamic analyses [13].

$$\alpha [M] + \beta [K] = [C] \quad (1)$$

The above equation represented the damping matrix [C], the mass matrix [M], the stiffness matrix [K], and the mass and stiffness coefficients, respectively. In the high-frequency range, damping proportional to stiffness predominates, whereas in the low-frequency range, damping proportional to mass predominates. The value of alpha coefficients was calculated to be 0.143 based on the notion that the Dominant Frequency of Tabas earthquakes is low.

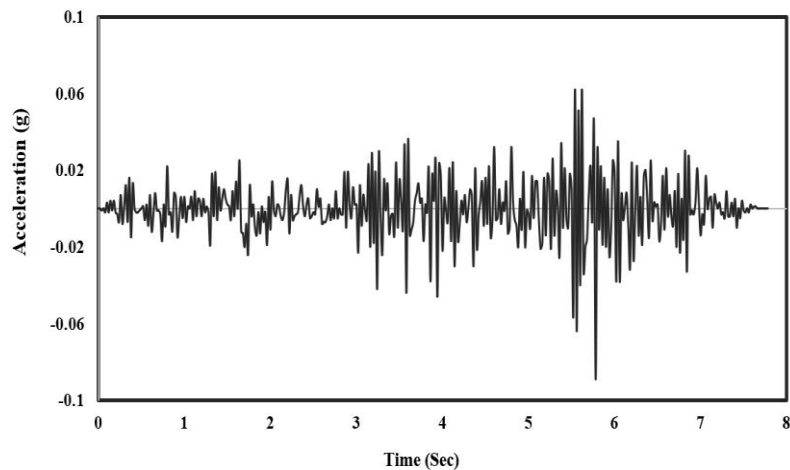


Figure 2. The Tabas earthquake accelerogram in the L-direction in terms of acceleration relative to gravity [14]

### 2.3. Mesh properties

Considering the size of the mesh has an important effect on the accuracy of the results in dynamic simulation, Kuhlemeyer and Lysmer suggested the following equation. Based on this equation, the mesh dimension in the FEM software must be less than  $\Delta l$  [15].

$$\Delta l \leq \lambda / 10 = C_s / (10f) \quad (2)$$

In this equation,  $\Delta l$  represents the maximum acceptable mesh length,  $C_s$  represents the shear wave velocity, and  $f$  represents the earthquake frequency. To calculate the dominant frequency of Tabas earthquake acceleration spectrum, Fourier analysis was performed in SeismoSignal software. Fourier analysis transform the signal from the time domain to the frequency domain and the dominant frequency component from the frequency spectrum provided by the software can be identified. This is typically the frequency at which the amplitude of the signal is highest.

The dominant frequency of the Tabas earthquake was 7.14 Hz, and the shear wave velocity was approximately 226 m/s. As a result, the mesh length cannot exceed 3.16 m. The modeling for this work was carried out, with an average mesh length of 2.5 m. Fig. 3 shows the mesh distribution on the D-shaped and circular tunnels. To have a very precise analysis, mesh has been refined in the near area of the tunnel.

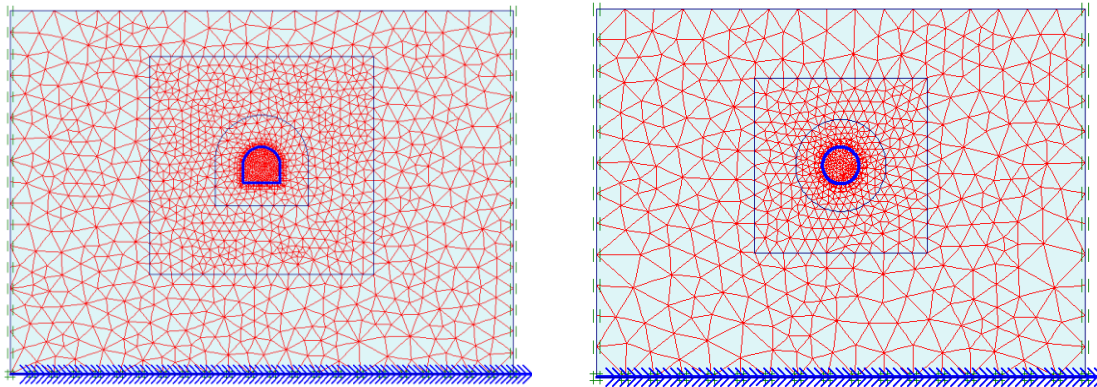


Figure 3. Mesh generation in D-shaped and Circular tunnels

### 2.4. Excavation patterns

Based on the findings, numerous methods have been proposed for the excavation pattern of tunnels, as illustrated in Figure 4. Each of these models conducted static analysis to compare the impact on ground settlement and the bending moment caused by the tunnel lining. Ultimately, only the most applicable cases have been subjected to dynamic and sensitivity analysis.

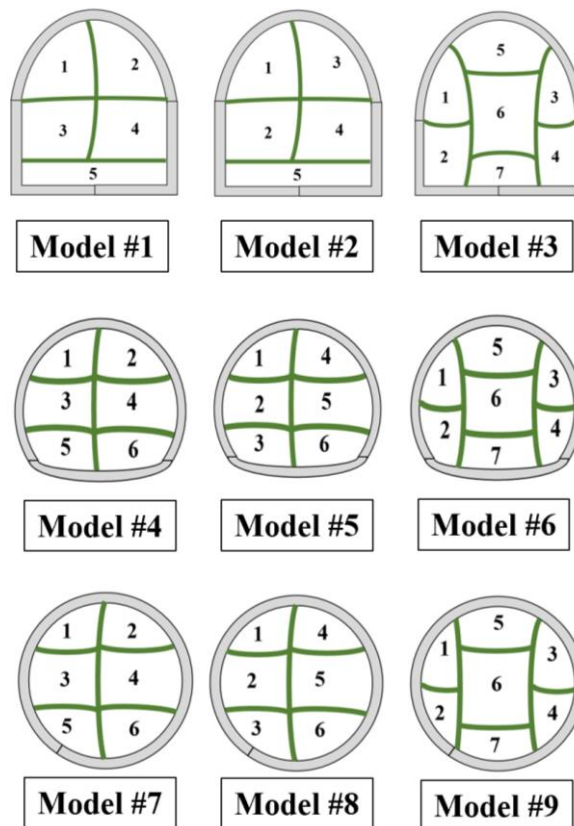


Figure4. The different patterns of excavation for D-shaped, horseshoe-shaped and circular tunnels.

## 2.5. Lining properties

In this study performed parametric analyses on three different types of tunnels: circular, horseshoe, and D-shaped tunnels. All tunnels were assumed to have an equal diameter of 8 meters and were located at the depth of 20 meters below ground level. Lining parameters of the tunnels are based on Tehran Metro Line 6 and are shown in Table 2.

Table 2. Tunnels lining properties[13]

| Type            | Model         | Modules of Elasticity (MPa) | Thickness (m) | Poisson Ratio | Unit Weight (Kg/m3) | Weight (KN/m2) | Rayleigh Alfa |
|-----------------|---------------|-----------------------------|---------------|---------------|---------------------|----------------|---------------|
| Concrete lining | Liner elastic | 30000                       | 0.4           | 0.25          | 2400                | 8.4            | 0.531         |

## 3-Methodology

Sensitivity analysis is performed to explain how material qualities impact the models and their output. In other words, sensitivity analysis examines how changing a specific parameter impacts the maximum bending moment exerted on the maintenance system while keeping the geotechnical parameters constant. In tunnels and underground spaces, the maximum bending moment imposed on lining systems and ground settlement are influenced by the tunnel's depth, unit mass, modules of elasticity, internal friction angle, and cohesion of the tunnel's surrounding soil. So in this research, sensitivity analysis on these important factors has been carried out. Sensitivity analysis is a method used to evaluate the stability of a system. In a system where characteristic P is governed mainly by n factors of  $\alpha = \{\alpha_1, \alpha_2, \alpha_3, \dots, \alpha_n\}$ ,  $P = f\{\alpha_1, \alpha_2, \alpha_3, \dots, \alpha_n\}$ .

Under a reference state of  $\alpha^* = \{\alpha_1^*, \alpha_2^*, \alpha_3^*, \dots, \alpha_n^*\}$  the character is described by P\*. The sensitivity analysis is to let the above individual factors vary within respective possible range and then analyze both tendency and extent to which the character of the system, P, departs from the base state due to the variation of the factors.

### 3.1. Sensitivity Analysis Method

The first step of sensitivity analysis is to establish the system model, i.e., the functional relation between the system character and the factors,  $P = f\{\alpha_1, \alpha_2, \alpha_3, \dots, \alpha_n\}$ . This relation should be, if possible, described by analytical expression. In the case of a complex system, it can be expressed by numerical method or through presentation of graphic chart. In dimensionless analysis, the sensitivity function and sensitivity factor are expressed using dimensionless expressions. The ratio of the relative error ( $\delta_P$ ) of the system character P ( $\delta_P = |\Delta P|/P$ ) to the relative error of parameter  $\alpha_k$  ( $\delta_{\alpha_k} = |\Delta \alpha_k|/\alpha_k$ ) is defined as the sensitivity function,  $S_k(\alpha_k)$ , of the parameter  $\alpha_k$  [16,17].

$$s_k(\alpha_k) \triangleq \frac{\left( \frac{|\Delta P|}{P} \right)}{\left( \frac{|\Delta \alpha_k|}{\alpha_k} \right)} = \left| \frac{\Delta P}{\Delta \alpha_k} \right| \frac{\alpha_k}{P} \quad k=1,2,3,\dots,n \quad (3)$$

When  $|\Delta \alpha_k|/\alpha_k$  is small, the function of  $S_k(\alpha_k)$  can be expressed approximately as [16,17]:

$$s_k(\alpha_k) = \left| \frac{d \phi_k(\alpha_k)}{d \alpha_k} \right| \frac{\alpha_k}{P} \quad k=1,2,3,\dots,n \quad (4)$$

From Eq. 4, the sensitivity function curve of  $\alpha_k$  can be obtained, which is shown in Fig. 5. Given  $\alpha_k = \alpha_k^*$ , the sensitivity factor  $S_k^*$  of the parameter  $\alpha_k$  is obtained as :

$$S_k^* = S_k(\alpha_k^*) = \left( \frac{d \phi_k(\alpha_k)}{d \alpha_k} \right) \alpha_k = \alpha_k^* \frac{\alpha_k^*}{P^*} \quad k=1,2,3,\dots,n \quad (5)$$

Where  $S_k^*$  and k are a group of dimensionless positive real numbers. Larger values of  $S_k^*$  indicate a greater sensitivity of parameter P to  $\alpha_k$ . By comparing different values of  $S_k^*$ , an assessment of the sensitivity of different parameters can be made[16,17].

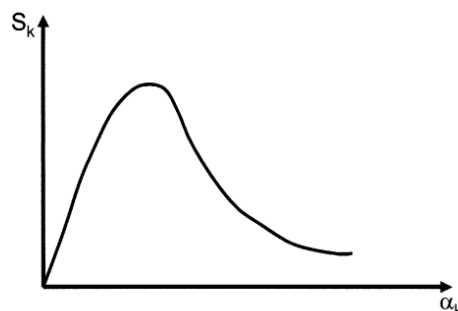


Figure 5. Curve of sensitivity function  $S_k - \alpha_k$  [17].

### 3.1. The input parameters of sensitivity analysis

Sensitivity analysis is carried out on the geotechnical parameters of unit weight, modulus of elasticity, internal friction angle, and cohesion of soil surrounding the tunnel in order to establish the maximum bending moment induced on the lining of the tunnel. The values of each of these parameters are regarded as 10%, 20%, or more, or less, than their reference values. Table 3 lists the input parameters for doing a sensitivity analysis based on the soil characteristics.

Table 3. The input Soil characteristics of sensitivity analysis

| Soil characteristics             | reference value [13] | Values of sensitivity analysis |
|----------------------------------|----------------------|--------------------------------|
| Unit weight (Kg/m <sup>3</sup> ) | 2000                 | 1600-1800-2200-2400            |
| Elastic modulus (MPa)            | 150                  | 120-135-165-180                |
| Cohesion (KPa)                   | 60                   | 48-54-66-72                    |
| Friction angle (degrees)         | 30                   | 24-27-33-36                    |

## 4- Results of static analysis

To identify the best pattern of excavation for tunnels, nine soil excavation models, as illustrated in Fig. 4, were studied in the static analysis phase, and the settlements and stresses acting on the support system for each excavation pattern were investigated.

Table 4 shows the result of static analysis on various shape of tunnels. According to table 4's findings, compared to D-shaped and Horseshoe-shaped tunnels, the amount of ground settlement, displacement of the tunnel roof, maximum bending moment, and maximum axial force of the tunnel's lining are lowest in circular tunnels. All the designs in a D-shaped tunnel exhibit almost the same ground settlement and tunnel ceiling displacement, however, pattern #3 exhibits the lowest bending moment and axial force. So in this research, further dynamic analysis in D-shaped tunnel should be performed based on static analysis in pattern #3.

Among the results of the static analysis in Horseshoe-tunnel models, patterns #4 and #6 show the lowest bending moment and axial force. But by comprising the results of the ground settlement and displacement of tunnel ceiling of all patterns, it is noticeable that model #6, shows the lowest values. So the results indicate that further dynamic analysis in Horseshoe-tunnel should be performed based on static analysis on pattern #6.

Finally, in a circular tunnel, pattern #9 indicates the lowest ground settlement and tunnel ceiling displacement. Furthermore, the bending moment value is almost the same for all excavation patterns. As a consequence of the findings, pattern #9 seems to be an adequate model, and additional dynamic study in a circular tunnel should be performed based on the static analysis of pattern #9.

In order to verify the accuracy of these numerical models, the final outcomes were compared with those of other researchers. Rostami and colleagues conducted a numerical research to analyze the impact of a tunnel's cross-sectional shape on the distribution of forces and settlements on the ground surface resulting from excavation activities. The study determined

that circular cross-section tunnels suffer lower forces compared to other cross-sections. Specifically, rectangular cross-section tunnels experience the highest forces under similar conditions. Furthermore, the findings of the conducted analysis indicate that the type of tunnel cross-section also has a substantial impact on the settlements that occur. It is important to note that, when exposed to similar environmental conditions and loading, the construction of a tunnel with a rectangular cross-section will result in a larger amount of settlement compared to tunnels with circular and horseshoe-shaped sections. Conversely, a tunnel with a circular cross-section will cause the least amount of settlement on the ground surface [18]. It is important to mention that their conclusions closely correspond to the outcomes of the numerical modeling carried out in this research.

To summarize, the results show that patterns #3, #6, and #9 typically demonstrate the least amount of displacements, bending moments, and forces imposed on tunnel lining compared to other excavation models. The implementation of pattern #3 can result in a 33% reduction in ground displacement compared to patterns #1 and #2 in D-shaped tunnels. Implementing patterns #6 and #9 can reduce ground displacements by approximately 40.7% and 22% in Horseshoe-shaped and Circular tunnels, respectively, compared to other excavation patterns. Furthermore, while comparing the bending moments in these three tunnel shapes, it can be concluded that the utilization of a circular tunnel results in a reduction of approximately 75% in the bending moment on the tunnel's lining. Similarly, employing a horseshoe-shaped tunnel leads to a reduction of around 54% in bending moment in comparison to a D-shaped tunnel.

**Table 4. Results of static analysis based on different excavation models**

| Parameters                                     | Excavation Models |      |      |                         |       |      |                 |      |      |
|--|-------------------|------|------|-------------------------|-------|------|-----------------|------|------|
|  | D-shaped tunnel   |      |      | Horseshoe-shaped tunnel |       |      | Circular tunnel |      |      |
|  | #1                | #2   | #3   | #4                      | #5    | #6   | #7              | #8   | #9   |
| Ground settlement (mm)                         | 7.85              | 6.22 | 5.23 | 8.06                    | 6.59  | 4.78 | 6.33            | 5.07 | 4.93 |
| Displacement of tunnel ceiling (mm)            | 30.2              | 26.2 | 23.7 | 31.3                    | 27.21 | 22.6 | 26.4            | 23.4 | 23.8 |
| Maximum bending moment of tunnel lining (kN.m) | 273               | 315  | 292  | 132                     | 145   | 136  | 79              | 83   | 73   |
| Maximum axial force of tunnel lining (kN)      | 327               | 369  | 347  | 353                     | 387   | 327  | 169             | 227  | 249  |

## 5- Results of the dynamic analysis

By varying geotechnical parameters like cohesion, friction angle, elasticity modulus, and unit weight of the surrounding soil of the tunnel, it was possible to investigate and analyze the sensitivity of the geotechnical parameters of the soil surrounding the tunnel on the bending moment induced in the tunnel lining under dynamic loads. The results of the bending moment created in the tunnel lining in the D-shaped tunnel, based on the input values in Table 3, are shown in Fig. 6. This figure shows the variation of the bending moment in terms of changes in cohesion, friction angle, unit weight, and elasticity modulus of soil surrounding of the tunnel.

Eq. 6 to Eq. 10 show the relationship between the maximum bending moment on the tunnel lining and each of the parameters based on the best-fit curve discovered from the numerical analysis findings (Fig. 6).

$$M_c = 0.0063c^2 - 1.4109c + 783.74 \quad (6)$$

$$M_\phi = -5.8893\phi + 903.95 \quad (7)$$

$$M_\rho = 0.1518\rho + 424.97 \quad (8)$$

$$M_E = -2.6933E + 1125.6 \quad (9)$$

Eq. 5 and the formulae mentioned above are used to generate the sensitivity function. By substituting the base values into the sensitivity function, the sensitivity factor  $M_c^*$ ,  $M_\phi^*$ ,  $M_\rho^*$ , and  $M_E^*$  are computed and Eq. 10 to Eq. 13, demonstrating the sensitivity of the specified parameters in each instance, respectively. The effects of each parameter can be identified by comparing them all. Due to the fact that the method is the same for other shapes of tunnels (circular and horseshoe), Fig 7 and Fig 8 show the relationship between the maximum bending moment on the tunnel lining and each of the parameters based on the best-fit curve discovered from the numerical analysis findings. The values and the summary of the sensitivity factors for the factors affecting the maximum bending moment on the tunnel lining are shown in Table 5.

$$M_c^* = \left| \frac{M_c}{d_c} \right| \frac{c}{M_{Max}} = \frac{(2 \times 0.0063c - 1.4109) \times c}{0.0063c^2 - 1.4109c + 783.74} = 0.99 \tag{10}$$

$$M_\phi^* = \left| \frac{M_\phi}{d_\phi} \right| \frac{\phi}{M_{Max}} = \frac{5.8893\phi}{-5.8893\phi + 903.95} = 0.242 \tag{11}$$

$$M_\rho^* = \left| \frac{M_\rho}{d_\rho} \right| \frac{\rho}{M_{Max}} = \frac{0.1518\rho}{0.1518\rho + 424.97} = 0.417 \tag{12}$$

$$M_E^* = \left| \frac{M_E}{d_E} \right| \frac{E}{M_{Max}} = \frac{2.6933E}{-2.6933E + 1125.6} = 0.735 \tag{13}$$

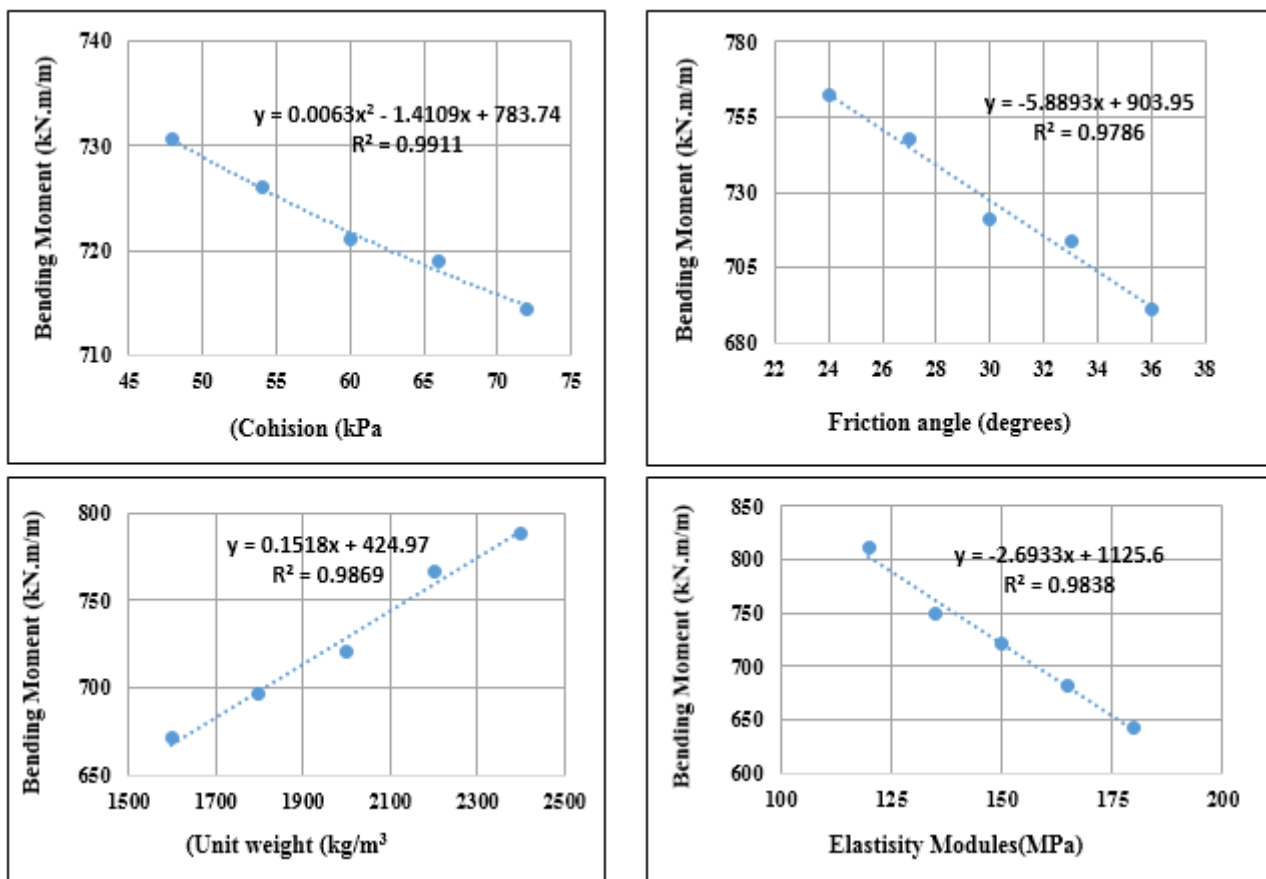


Figure 6. Variations of the bending moment on the tunnel lining in terms of changes in cohesion, friction angle, elasticity modulus and unit weight for D-shaped tunnel

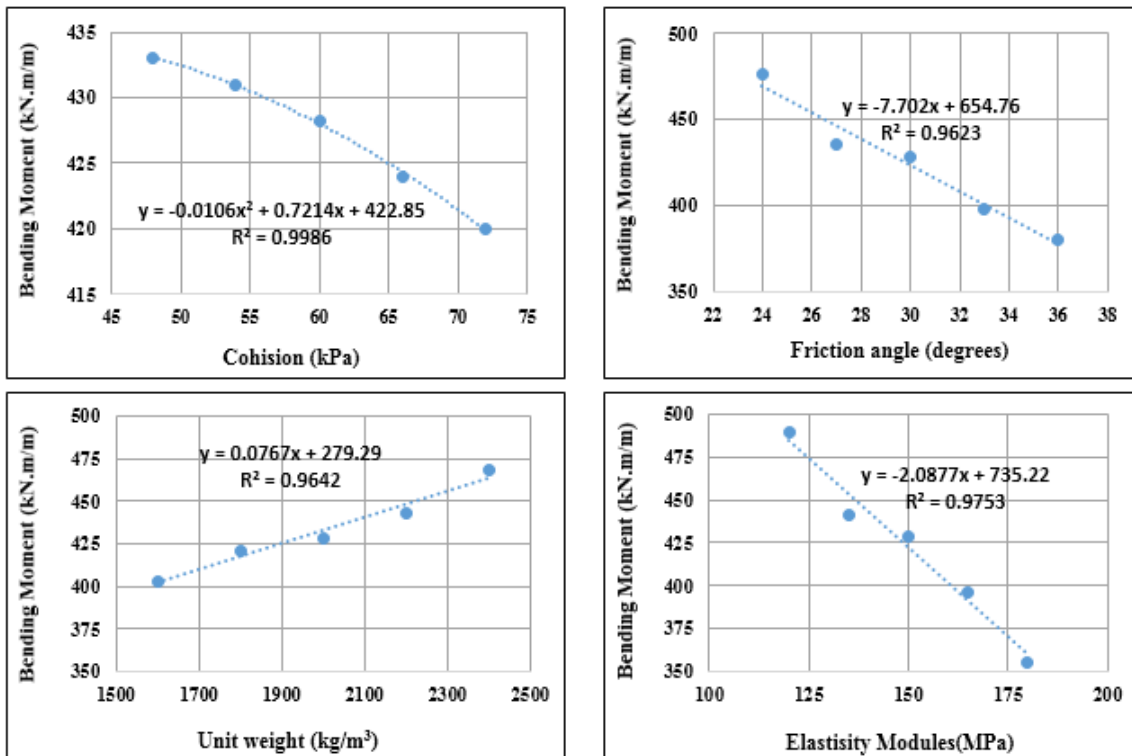


Figure 7. Variations of the bending moment on the tunnel lining in terms of changes in cohesion, friction angle, elasticity modulus and unit weight for Horseshoe-shaped tunnel

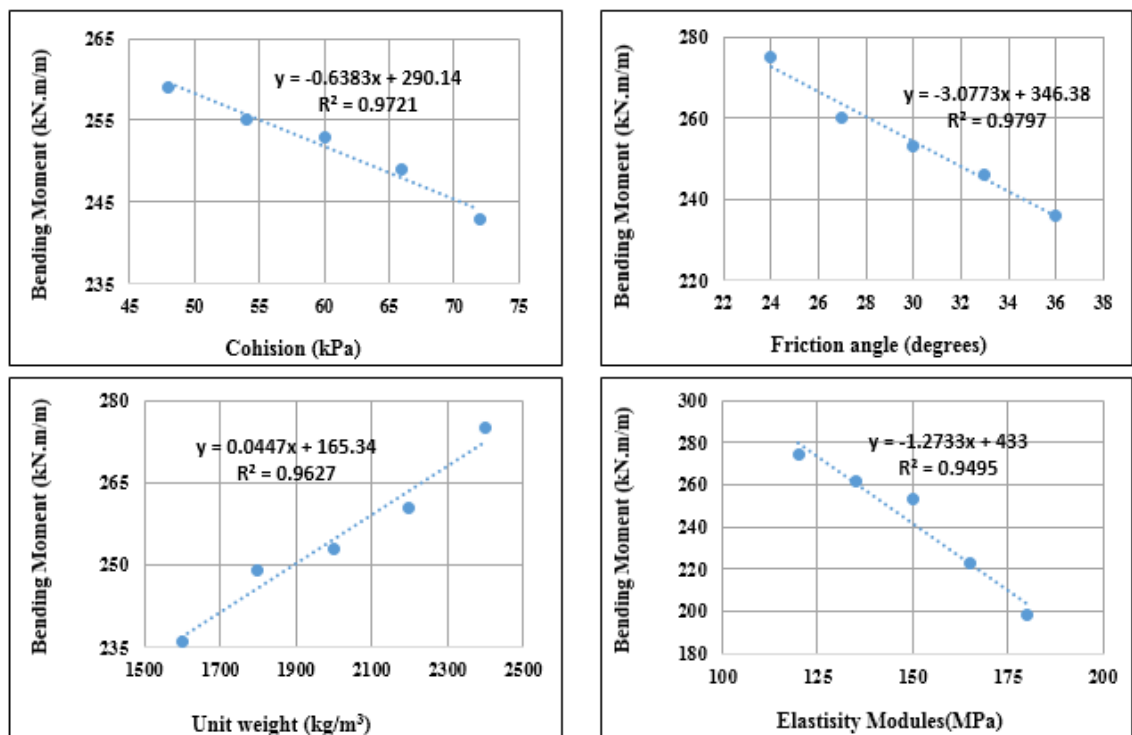


Figure 8. Variations of the bending moment on the tunnel lining in terms of changes in cohesion, friction angle, elasticity modulus and unit weight for Circular tunnel

Table 5. Results of the sensitivity analysis on the geotechnical parameters of the tunnel's soil surrounding

| Sensitivity Factor | Tunnels shape   |                         |                 |
|--------------------|-----------------|-------------------------|-----------------|
|                    | D-shaped tunnel | Horseshoe-shaped tunnel | Circular tunnel |
| $M_c^*$            | 0.099           | 0.279                   | 0.156           |
| $M_\phi^*$         | 0.242           | 0.54                    | 0.36            |
| $M_\rho^*$         | 0.417           | 0.331                   | 0.458           |
| $M_E^*$            | 0.735           | 0.742                   | 0.789           |

According to Fig. 6 to Fig. 8, in all shape of tunnels, the maximum bending moment on the tunnel lining induced by seismic waves, increases with an increase in unit weight but decreases with rises in cohesion, internal friction angle, and elasticity modulus of the soil surrounding of tunnels.

Table 5 shows that the elasticity modulus of the soil surrounding tunnels has the greatest sensitivity factor. This implies that, among soil properties, the stiffness of the soil surrounding the tunnel has a considerable influence on the stability of the tunnel, especially during seismic conditions. It is also noticeable that, because of the lowest sensitivity factors, cohesion value of the soil surrounding of tunnel has the least impact on bending moment induced on tunnel's lining. Also, changes in the unit weight and internal friction angle, which are next in significance, may also have a small influence on the maximum bending moment.

In this regard, Fig. 9 depicts the percentage contribution of various geotechnical parameters of the soil surrounding the tunnel on the bending moment induced in its lining. Variations in the elastic modulus (stiffness) have the greatest impact on the changes in the bending moment induced in the tunnel lining. Approximately 73.5%, 74.2%, and 78.9% affect the magnitude of the bending moment in the D-shaped, horseshoe, and circular tunnels, respectively in comparison to other geotechnical parameters. Also, the percentage of sensitivity factors of unit weight are 41.4%, 33% and 45.8% in the D-shaped, horseshoe, and circular tunnels and for friction angle are 24.2%, 54% and 36% and finally for cohesion are 9.9%, 27.9% and 15.6% respectively.

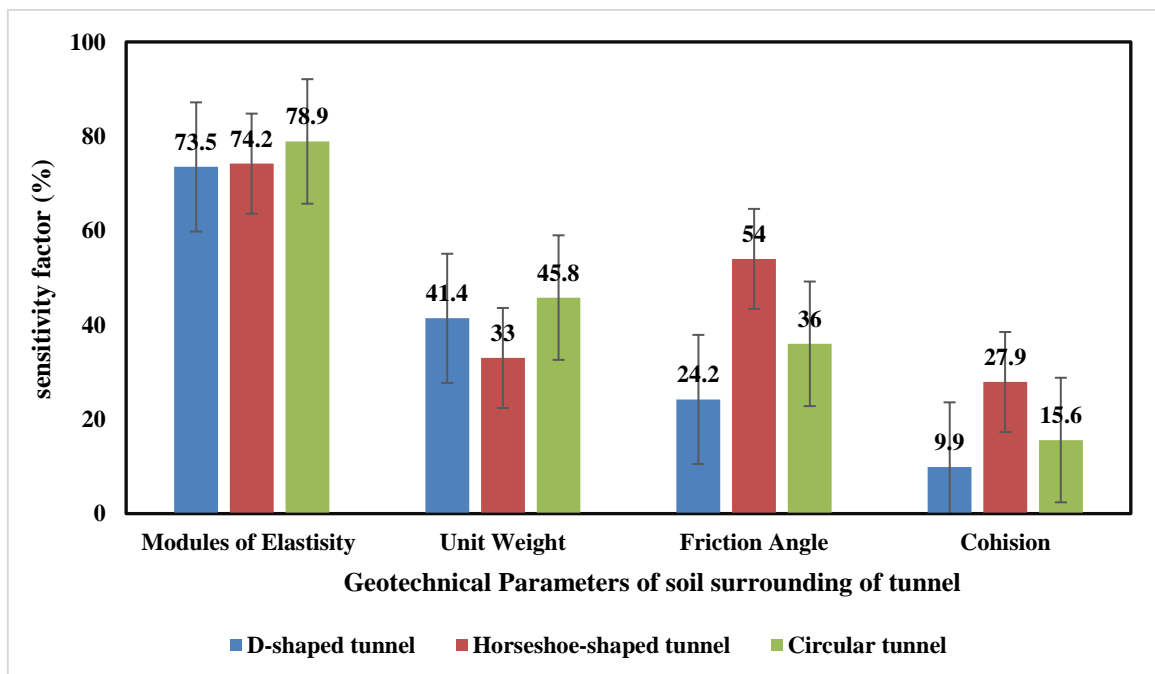


Figure 9. Results of the sensitivity factor of the geotechnical parameters soil surrounding the tunnel in induced bending moment on tunnel lining

In order to verify the accuracy of these numerical models, the final outcomes were compared with those of other researchers. In this regard, Santos and et al. conducted similar studies on a tunnel with a diameter of 10 meters and positioned at a depth of 15 meters using the two-dimensional FLAC software to investigate the influence of soil parameters around the tunnel on the forces and moments acting on the tunnel lining. In their analyses, they varied the soil cohesion from 20 to 196 kPa, the soil friction angle from 10 to 30 degrees, the unit weight of the soil from 18 to 21, and the soil elasticity modulus from 54 to 110 MPa in a sensitivity analysis, and obtained the axial force and bending moment acting on the tunnel lining. By examining these studies, it can be stated that an increase in the values of the cohesion, friction angle, and elasticity modulus of the soils surrounding the tunnels leads to a reduction in the axial force and bending moment in their linings, but an increase in the specific weight of the soil has the opposite effect. Furthermore, the influence of the soil elasticity modulus on the forces and bending moments of the tunnel is greater than the other parameters [19].

Also, Hamrouni and et.al evaluated the performance of a shallow circular tunnel by considering the soil spatial variability. They conducted research within multiple probabilistic analyses by using (FLAC2D) software. They concluded that the main input parameters that have a significant effect on the lining bending moments are the soil elastic parameters, for the settlements, mainly the elastic parameters and the soil unit weight have a significant effect [20]. Ultimately, it should be noted that their studies are highly correlated with the results of this research.

## 6- Summary and Conclusion

This study investigated the effective factors in reducing earthquake damages in tunnels and underground structures. For this purpose, sensitivity dynamic analysis (based on Tabas earthquake acceleration spectrum) on geotechnical parameters of the soil surrounding tunnel such as cohesion, friction angle, unit weight and modulus of elasticity was carried out, and the parameters whose changes have the greatest and least effects on the bending moment changes on the tunnel lining are introduced. According to results of FEM analysis, the following general conclusions can be drawn from this study:

1. It can be concluded that tunnel excavation patterns significantly affect the bending moment, axial forces, displacements, and surface settlement of the tunnel. Often by dividing tunnel excavation's area to small sections, the values of bending moment, axial forces, displacements, and surface settlement of the tunnel, decrease in static analysis.
2. The shape of the tunnels has the significant impact on the bending moment and axial force on the tunnel lining. The research's findings demonstrated that, in D-shaped tunnels, the bending moment and axial force values are much higher than the circular and horseshoe tunnels.
3. Results of the static analysis show that patterns #3, #6, and #9 typically demonstrate the least amount of displacements, bending moments, and forces imposed on tunnel lining compared to other excavation models. The implementation of pattern #3 can result in a 33% reduction in ground displacement compared to patterns #1 and #2 in D-shaped tunnels. Implementing patterns #6 and #9 can reduce ground displacements by approximately 40.7% and 22% in Horseshoe-shaped and Circular tunnels, respectively, compared to other excavation patterns.
4. Results of the static analysis that utilization of a circular tunnel results in a reduction of approximately 75% in the bending moment on the tunnel's lining. Similarly, employing a horseshoe-shaped tunnel leads to a reduction of around 54% in bending moment in comparison to a D-shaped tunnel.
5. The bending moment of tunnel's lining is decreased by increasing the amount of cohesion, friction angle, and elasticity modulus of the soil surrounding the tunnel. But the maximum bending moment rises as the unit weight of earth around the tunnel increases.
6. The results demonstrated that, among the geotechnical characteristics of soil surrounding of tunnel, changes in the elasticity modulus have the greatest impact on changes in the bending moment for each of the D-shaped, Horseshoe-shaped and circular shaped tunnels and approximately 73.5%, 74.2%, and 78.9% affect the magnitude of the bending moment in the D-shaped, horseshoe, and circular tunnels, respectively in comparison to other geotechnical parameters.
7. Changes in the cohesion of the soil surrounding the tunnels have the least impact on the bending moment under dynamic loading and just 9.9 %, 27.9 % and 15.6 % affect the magnitude of the bending moment in the D-shaped, horseshoe, and circular tunnels, respectively in comparison to other geotechnical parameters.

## References

1. Asheghi Mehmandari, T., Fahimifar, A., & Asemi, F. (2020). The Effect of the Crack Initiation and Propagation on the P-Wave Velocity of Limestone and Plaster Subjected to Compressive Loading. *AUT Journal of Civil Engineering*, 4(1), 55-62. <https://doi.org/10.22060/ajce.2019.15984.5558>
2. Zare, P., Asheghi, T., Fahimifar, A., & Zabetian, S. (2020). Experimental Assessment of Damage and Crack Propagation Mechanism in Heterogeneous Rocks.
3. Asakura, T., Sato, Y. (1998). "Mountain tunnels damage in the 1995, HYOOKEN-NANBU Earthquake", *QUARTERLY REPORT-RTRI*, 39, P. 9-16.
4. Cui, C., Cheng, X., Sun, Z., & Xu, C. (2017). Analysis of seismic response and parametric sensitivity of subway station surrounded by saturated soft soil. *Journal of Railway Engineering Society*, 34, 92-98.
5. Cilingir, U., & Madabhushi, S. P. G. (2017). Effect of depth on seismic response of circular tunnels. *Canadian Geotechnical Journal*, 48, T10-047.
6. Nahhas, F., Tawfik, A., & Motaal, M. (2006). Engineering Safety of Tunnels During Earthquakes. *Journal of Soil and Foundation*, 46, 737-748.
7. Nahhas, F., Tawfik, A., & Motaal, M. (2013). Mutual seismic interaction between tunnels and the surrounding granular soil. *HBRC Journal*, 9, 265-278.
8. Madabhushi, S. P. G., & Cilingir, U. (2011). A model study on the effects of input motion on the seismic behaviour of tunnels. *Soil Dynamics and Earthquake Engineering*, 31, 452-462.
9. Naserkhaki, S., & Vafaeian, M. (2006). Study of Tunnel Response to Seismic Loads Corresponding to Different Values of Depth and PGA.
10. Chen, C. H., Wang, T. T., Jeng, F. S., & Huang, T. H. (2012). Mechanisms causing seismic damage of tunnels at different depths. *Tunnelling and Underground Space Technology*, 28, 31-40.
11. Liu, C. Q., Fu, W. Q., Luo, W., Liu, D., & Sun, Y. (2020). Sensitivity Analysis Of Influencing Factors On Tunnel Stability In Bad Geological Slope Sections. *E3S Web Conf.*, 145, 02049. doi: 10.1051/e3sconf/202014502049
12. Vo-Minh, H. C. Nguyen. (2022). Seismic stability of a circular tunnel in cohesive-frictional soils using a stable node-based smoothed finite element method. *Tunneling and Underground Space Technology*, 130.
13. Shirizadeh, H., & Dehghan, S. (2017). Determination of the optimal distance of non-planar cross tunnels using numerical method –A case study of the intersection of Tehran Metro Lines 6 and 7. *10.22044/tuse.2017.4585.1274*
14. Pacific Earthquake Engineering Research Center (PEER) ground motion database
15. Kuhlemer, R. L., & Lysmer, J. (1973). Finite Element Method accuracy for wave propagation problems. *Journal of Soil Mechanics and Foundation Division*, 99, 421-427.
16. Zhao, J., & Zhu, W. (2004). Stability analysis and modelling of underground excavation in fractured rocks. Elsevier Geo-Engineering Book Series (Vol. 1).
17. Bedford, T., & Cooke, R. (2001). Probabilistic Risk Analysis: Foundations and Methods. Cambridge, UK: Cambridge University Press.
18. Rostami, A., Asghari, N., & Shahi, B. (2016). Investigation Effect of Tunnel Gate Shapes with Similar Cross Section on Inserted Forces on Its Coverage and Soil Surface Settlement. *Open Journal of Civil Engineering*, 6, 358-369.
19. Hamrouni, A.; Dias, D.; Guo, X. Behavior of Shallow Circular Tunnels—Impact of the Soil Spatial Variability. *Geosciences* 2022, 12, 97. <https://doi.org/10.3390/geosciences12020097>
20. Santos, C.D., Villalba, A.L., & Morancho, A.L. (2009). Effect of soil saturation changes on pressure on tunnel linings, *Engineering, Environmental Science*.